Differentiation of osteoclast precursors on Gellan Gum-based spongy-like hydrogels for bone tissue engineering

To cite this article before publication: Raquel Maia *et al* 2018 *Biomed. Mater.* in press https://doi.org/10.1088/1748-605X/aaaf29

Differentiation of osteoclast precursors on Gellan Gum-based spongy-like hydrogels for bone tissue engineering

F. Raquel Maia[1,2,*], David S. Musson[3], Dorit Naot[3], Lucilia P. da Silva[1,2], Ana R. Bastos[1,2], João B. Costa[1,2], Joaquim M. Oliveira[1,2,4], Vitor M. Correlo[1,2,4], Rui L. Reis[1,2,4] and Jillian Cornish[3]

[1]3B's Research Group - Biomaterials, Biodegradables and Biomimetics, University of Minho, Headquarters of the European Institute of Excellence on Tissue Engineering and Regenerative Medicine, Avepark – Parque de Ciência e Tecnologia, Zona Industrial da Gandra, 4805-017 Barco GMR-Portugal.

[2]ICVS/3B's - PT Government Associated Laboratory, Braga, Portugal.

[3]Department of Medicine, University of Auckland, Auckland, New Zealand.

[4]The Discoveries Centre for Regenerative and Precision Medicine, Headquarters at University of Minho, Avepark, 4805-017 Barco, Guimarães, Portugal

*Corresponding author: F. Raquel Maia (raquel.maia@dep.uminho.pt)

Abstract

Bone tissue engineering with cell-scaffold constructs has been attracting a lot of attention, in particular as a tool for efficient guiding of new tissue formation. However, the majority of the current strategies used to evaluate novel biomaterials focus on osteoblasts and bone formation, while osteoclasts are often overlooked. Consequently, there is limited knowledge about the interaction between osteoclasts and biomaterials. In this study, the ability of gellan gum and hydroxyapatite reinforced gellan gum spongy-like hydrogels to support osteoclastogenesis was investigated *in vitro*. First, gellan gum and hydroxyapatite reinforced gellan gum spongy-like hydrogels were characterized in terms of microstructure, water uptake and mechanical properties. Then, bone marrow cells isolated from mice long bones and cultured in the spongy-like hydrogels were treated with 1,25-dihydroxyvitamin D3 to promote osteoclastogenesis. It was shown that the addition of HAp to Gellan Gum spongy-like hydrogels enables the formation of lager pores and thicker walls, promoting an increase in stiffness. hydroxyapatite reinforced gellan gum spongy-like hydrogels supported the formation of aggregates of tartrate-resistant acid phosphatase-stained cells and the expression of the genes encoding DC-Stamp and Cathepsin K, suggesting the differentiation of bone marrow cells into pre-osteoclasts. The hydroxyapatite reinforced gellan gum spongy-like hydrogels developed in this work show promise for future use in bone tissue scaffolding applications.

Keywords: Bone tissue engineering; Osteoclastogenesis; Spongy-like hydrogels; 3D scaffolds; Hydroxyapatite.

1. Introduction

Tissue engineering strategies for the repair and regeneration of damaged bone tissues are being pursued by many research groups [1-3]. In this approach, biomaterials can be used as temporary vehicles for cell transplantation or recruitment and release of biologically active agents, aiming to guide new bone tissue formation [4-6]. Most studies of cell-transplanted biomaterials have focused on the development of new bone using mature osteoblasts or stem cells differentiated into osteoblasts [7, 8]. Nevertheless, bone is a highly dynamic and complex tissue, which renews through a process that involves not only osteoblasts for tissue formation, but also osteoclasts for tissue resorption. In fact, successful biomaterials for bone replacement should provide support to both osteoblasts and osteoclasts to enable the interactive process of bone remodeling, ensuring scaffold resorption and new bone formation [3].

Osteoclasts are multinucleated cells that develop from mononuclear macrophage/monocyte-lineage hematopoietic precursors and are essential for bone regeneration at sites of bone defects [9]. There is limited knowledge about interaction between osteoclasts and biomaterials, and the role osteoclast play in scaffold resorption[10]. Previous studies have shown that topography of the scaffold [11], and the chemical composition of its surface affect osteoclast activity [12]. Furthermore, it was shown that the production of wear particles from orthopedic implants stimulates the development of osteoclasts, resulting in implant loosening [13]. Hydroxyapatite (HAp)-based materials have favored osteoclast formation when compared with other calcium phosphate ceramics used for bone tissue regeneration, such as octacalcium phosphate (structurally similar with hydroxyapatite) [14], or β-tricalcium phosphate (β-TCP) [15].

Nevertheless, only a limited number of studies have focused on the interaction of osteoclasts with naturally-derived polymers such as Gellan gum, collagen, and silk fibroin [16-18]. These widely used biomaterials are similar to the extracellular matrix, have controlled degradation rate, and good biological performance for bone tissue regeneration. It has been shown that monocytes preferentially differentiated in scaffolds prepared using naturally-derived polymers, such as fibroin or chitosan, as compared with scaffolds prepared with synthetic polymers, namely poly(L-lactic acid) (PLLA) [17]. On the other hand, Kai and colleagues have shown that biphasic mineralized collagen scaffold (BCS) negatively regulated osteoclastogenesis and were detriment to osteogenesis [16].

Gellan gum (GG) is a polysaccharide produced by bacteria from the *Sphingomonas* group, composed of L-rhamnose, D-glucuronic acid and two D-glucose subunits [19]. GG forms hydrogels *in situ* by reacting with multivalent cations and resembles extracellular glycosaminoglycan composition [20-22]. A recent study described a simple method of modifying the characteristics of GG hydrogels, producing spongy-like hydrogels with improved cell adhesive and mechanical properties, which could be fine-tuned in order to fulfil the demands of each desired application [23].

GG degrades over time, ranging from weeks to months [24-26], an attractive characteristic for tissue regeneration of bone [2, 27-29], cartilage [30] and intervertebral disc repair [31]. Different strategies were pursued in order to develop GG matrices that can be used for bone tissue engineering. Among them, special attention was given to the mimicry of some of the native characteristics for the support of tissue formation/remodeling [26]. For example, Gantar *et al.* tailored GG spongy-like hydrogels properties by strengthening it with bioactive glass particles

[27]. These hydrogels allowed the formation of a mineral layer on their surface, enhancing the cytocompatibility. In a different approach, Douglas *et al*. integrated the enzyme alkaline phosphatase into the GG hydrogel to induce the formation of a mineral layer and improve mechanical strength and cellular interactions [2]. With the same intent, Jamshidi and colleagues modified GG with hydroxyapatite (HAp), improving the mechanical properties of the scaffold and osteogenesis [28]. To the best of our knowledge, no studies have investigated the GG spongy-like hydrogels' resorption and their capacity to support osteoclastogenesis.

In this work, the capacity of GG and hydroxyapatite reinforced GG (GG-HAp) spongy-like hydrogels to support osteoclastogenesis was evaluated *in vitro*. The microstructure, water uptake and mechanical properties of the hydrogels were determined as well as their ability to support osteoclastogenesis in cultures of 1,25-dihydroxyvitamin D3 (Vitamin D3)-treated murine bone marrow cells.

2. Material and methods

2.1. Gellan gum (GG) and hydroxyapatite reinforced gellan gum (GG-HAp) spongy-like hydrogels preparation and characterization

2.1.1. GG and GG-HAp spongy-like hydrogels preparation

The method used for the preparation of gellan gum (GG) and hydroxyapatite reinforced gellan gum (GG-HAp) spongy-like hydrogels is similar to the described elsewhere [23, 27]. In more detail,

precursor GG and GG-HAp hydrogels were prepared by dissolving Gelzan powder (Sigma-Aldrich, Missouri, USA) in deionized water at 90°C, at a final concentration of 1.25 wt% and under constant agitation. The solution was then cooled down to 60°C. At this point, for the preparation of GG-HAp hydrogels, HAp powder (Plasma Biotal, Buxton, UK) was added to a final concentration of 10% w/v. The solution was allowed to stand for 15 minutes at 60°C to obtain a homogeneous distribution of HAp. Then, both (GG and GG-HAp) solutions were crosslinked with calcium chloride ($CaCl_2$, Sigma-Aldrich, Missouri, USA) and casted into molds. After 30 minutes of stabilization, precursor GG and GG-HAp hydrogels were obtained. Discs of 8 mm of diameter and 3 mm of thickness were cut out and stored in phosphate-buffered saline (PBS Sigma-Aldrich, Missouri, USA) for a further stabilization period of 48 hours. Finally, to produce dried networks, hydrogel discs from both compositions were frozen overnight at −80°C for 18-20 hours and then, freeze-dried (CryoDos -80, Telstar, Terrassa, Spain) for 3 days to generate GG and GG-HAp dried polymeric networks (DPNs). Spongy-like hydrogels were formed after re-hydration of the DPNs.

2.1.2. Microstructure characterization

The microstructure of GG and GG-HAp dried polymeric networks (DPNs) was analyzed by micro-computed tomography (Micro-CT) and scanning electron microscopy (SEM). For Micro-CT, the DPNs samples were analyzed in an X-ray microtomography system Skyscan 1272 (Bruker, Kontich, Belgium) in a high-resolution mode using a pixel size of 11.31 µm and integration time of 1.7 s. The X-ray source was set at 35 keV of energy and 215 µA of current. Representative data sets of 150 slices were transformed into a binary picture using a dynamic threshold of 45e255

(gray values) to distinguish polymer material from pore voids. These data were used for morphometric analysis, which included quantification of the pore wall thickness, pore size and porosity. In the case of SEM, DPNs were analysed by scanning electron microscopy (JSM-6010 LV, Tokyo, Japan) at a 15 kV operating voltage after gold sputter-coating.

2.1.3. Water uptake

For water uptake analysis, DPNs were measured (Wd), immersed in PBS and incubated for 48 hours at 37°C. Then, at each time point (0.5, 1, 3, 7, 24 and 48 hours), each sample was measured again (Ww) and the percentage of water uptake along the time was calculated as follow: *Water uptake (%) = (Ww – Wd)/Wd × 100*.

2.1.4. Dynamic mechanical analysis (DMA) of spongy-like hydrogels

The viscoelastic measurements of spongy-like hydrogels (8 mm diameter; h= 6 mm) were performed using a TRITEC8000B dynamic mechanical analyzer (Triton Technology, Lincolnshire, UK). The spongy-like hydrogels were pre-equilibrated ON at 37°C in alpha-MEM (Alfagene, Carcavelos, Portugal) and then loaded onto the compression mode clamp assembly. The measurements were carried out at 37°C whilst immersed in a bath composed of PBS placed in a Teflon reservoir. A small preload was applied to each specimen to ensure adequate contact between the swollen specimen and the device. The DMA spectra were obtained during a frequency scan between 0.1 and 10 Hz. The experiments were performed under a constant strain

amplitude (50 μm). The average values at a frequency of 1 Hz for the compressive storage modulus (*E'*, elastic component) and tan δ (loss-to-storage modulus ratio) of swollen spongy-like hydrogel were calculated. The influence of HAp on the spongy-like hydrogels' mechanical properties was analyzed. A minimum of three specimens were used for each condition. Averages and standard deviations were reported.

2.2. Cell culture

2.2.1. Isolation of bone marrow cells

Bone marrow was obtained from long bones of male CD-1 mice aged 4–6 weeks. All protocols were approved by the Animal Ethics Committee at the University of Auckland. Bone marrow cells were isolated as described previously [32]. Briefly, femurs and tibias were removed and dissected free of adhering tissues. The epiphyses were cut off and the marrow cavity was flushed with alpha-MEM using a syringe with a needle. The marrow cells were collected, spun at 1200 rpm for 2 minutes, and washed with alpha-MEM containing 10% FBS (Alfagene, Carcavelos, Portugal). Marrow cells were then cultured for 2 hours in 90 mm Petri dishes. After 2 hours, nonadherent cells were collected, spun at 1200 rpm for 2 minutes, washed with 10% FBS/alpha-MEM, and used in subsequent studies. The resulting cultures are therefore depleted of mature osteoclasts.

2.2.2. 2D standard culturing of bone marrow cells

Bone marrow cells were seeded in standard 2D conditions at $0.5x10^6$ cells/cm^2 in 48-well plates in 10% FBS/alpha-MEM (hereafter designated as 2D cultures). In order to induce osteoclastogenesis, 2×10^{-8} M of 1,25-dihydroxyvitamin D_3 [$1,25(OH)_2D_3$] (Vitamin D3, Calbiochem, Massachusetts, USA) [33] was added on days 0, 2 and 4. Cultures without Vitamin D3 were used as control. Cultures were maintained at 37°C under a humidified atmosphere of 5% (v/v) CO_2 in air.

2.2.3. 3D culturing on GG and GG-HAp spongy-like hydrogels

GG and GG-HAp spongy-like hydrogels were sterilized by ethylene oxide prior to cell seeding. A drop (30 µL) of bone marrow cells' suspension was seeded on top of the GG and GG-HAp dried polymeric networks at $1x10^6$ cells/cm^2 in 10% FBS/alpha-MEM. After 30 minutes, the dried polymeric network absorbed the cells' suspension, entrapping BM cells inside, and formed spongy-like hydrogels. Cultures were maintained in 48 -well plates, pre-treated with poly (2-hydroxyethyl methacrylate) (pHEMA, Sigma-Aldrich, Missouri, USA, 10% v/v in ethanol 95%) to avoid cell adhesion to the bottom of the plates. To induce osteoclastogenesis, 2×10^{-8} M of Vitamin D3 was added on days 0, 2 and 4. Cultures without Vitamin D3 were used as control. Cultures were maintained at 37°C under a humidified atmosphere of 5% (v/v) CO_2 in air.

2.2.4. Tartrate-resistant acid phosphatase (TRAP) staining

After 7 days of culture, cells were fixed with a solution of 37% formaldehyde (Sigma-Aldrich, Missouri, USA), acetone (VWR, Leuven, Belgium), and 0.01 M sodium citrate buffer (Fisher Scientific, Hampshire, EUA) (pH 6.0) at the ratio of 1:8.1:3.1. To visualize osteoclasts, a staining for tartrate-resistant acid phosphatase (TRAP) was performed using a commercially Acid Phosphatase, Leukocyte (TRAP) Kit (Sigma-Aldrich, Missouri, USA). The staining was used to select the spongy-like hydrogels (GG or GG-HAp) that showed the most promising results for subsequent experiments. Images were obtained using a digital camera Olympus DP72 coupled to a microscope Olympus CKX41 (Olympus, Tokyo, Japan) in case of 2D cultures and a stereoscope Olympus SZ (Olympus, Tokyo, Japan) in the case of 3D cultures.

2.2.5. Cell viability assay

Cell viability was assessed using the Live/Dead™ (Molecular Probes™, Oregon, USA) assay and measuring metabolic activity through AlamarBlue® (Thermo Fisher Scientific, New Hampshire, USA) assay, at days 4 and 7. For Live/Dead™ assay, 2D and 3D cultures were washed with PBS and then incubated (10 minutes, 37°C in the dark) with calcein AM (4 µM, live cells) and ethidium homodimer-1 (EthD-1, 1 µM, dead cells) and washed again with medium. Samples were imaged by Olympus CKX41 microscope fitted with a digital camera Olympus DP72. For AlamarBlue® assay, 2D and 3D cultures were washed with PBS. Then, 10% of AlamarBlue in culture medium was added and incubated (3 hours, 37°C in the dark). The supernatant was then transferred to a 96-well plate and fluorescence measurements were carried out using a microplate reader (Biotek

Synergy MX, Vermont, USA) with Ex/Em at 530/590 nm. Cell viability assays were performed in triplicate.

2.2.6. Gene expression

Total RNA was extracted from bone marrow cells recovered from 2D and 3D cultures (n = 4) at day 0 and 7, using TRIzol® Reagent followed by Direct-zol™ RNA MiniPrep (Zymo Research, California, USA), as recommended by the manufacturer. RNA quantification was performed by using a NanoDrop spectrophotometer. Subsequently, 100 ng of the total RNA were used to generate single-stranded cDNA by random priming with SuperScript III reverse transcriptase (Invitrogen, California, USA). Multiplex real-time PCRs were carried out in a 384-well optical reaction plate in ABI PRISM 7900HT sequence detection system (Applied Biosystems, California, USA). VIC-labeled 18S rRNA, used as endogenous control, and FAM-labeled probes specific for the genes of interest were purchased as TaqMan gene expression assays. All reactions were performed in triplicate. The expression value for each sample was calculated using the $2^{-\Delta\Delta Ct}$ method, with the target value normalized to the 18S rRNA value and presented relative to the expression on day 0. All real-time PCR reagents used were from Applied Biosystems. Gene expression assays were performed in triplicate.

2.3. Statistical analysis

Statistical analyses were performed using GraphPad Prism 5.0. *T*-test was used to determine statistical significance of differences between the two experimental groups. Two-way ANOVA analysis was used every time that studies involved two independent variables. The critical level of statistical significance was $p<0.05$. Data are presented as mean ± standard deviation. Data in each figure are from a representative experiment of the triplicates performed with n=3 each.

3. Results

3.1. Physicochemical properties of GG and GG-HAp spongy-like hydrogels

3.1.1. *GG and GG-HAp dried polymeric networks' microstructure*

The microstructure and topography details of developed GG and GG-HAp dried polymeric networks was assessed by Micro-CT and SEM techniques (Figure 1). In representative pictures obtained by Micro-CT analysis (Figures 1(b), (e)) it was possible to observe differences in the microstructure, namely pore wall thickness and pore size, between GG and GG-HAp dried polymeric networks, which were further corroborated by morphometric analysis (Figures 1(g), (h)). GG-HAp dried polymeric networks showed higher pore sizes (≈ 1.5 times larger) and thicker pore walls (≈ 2 times thicker) than GG dried polymeric networks. It is important to mention that the combination of GG with HAp did not affect the porosity, resulting in similar values (≈ 50%) when comparing GG and GG-HAp dried polymeric networks (Figure 1(j)). Moreover, as depicted

in Figure 1(c), GG dried polymeric networks presented a smooth surface, while GG-HAp dried polymeric networks (Figure 1(f)) showed a rugged surface.

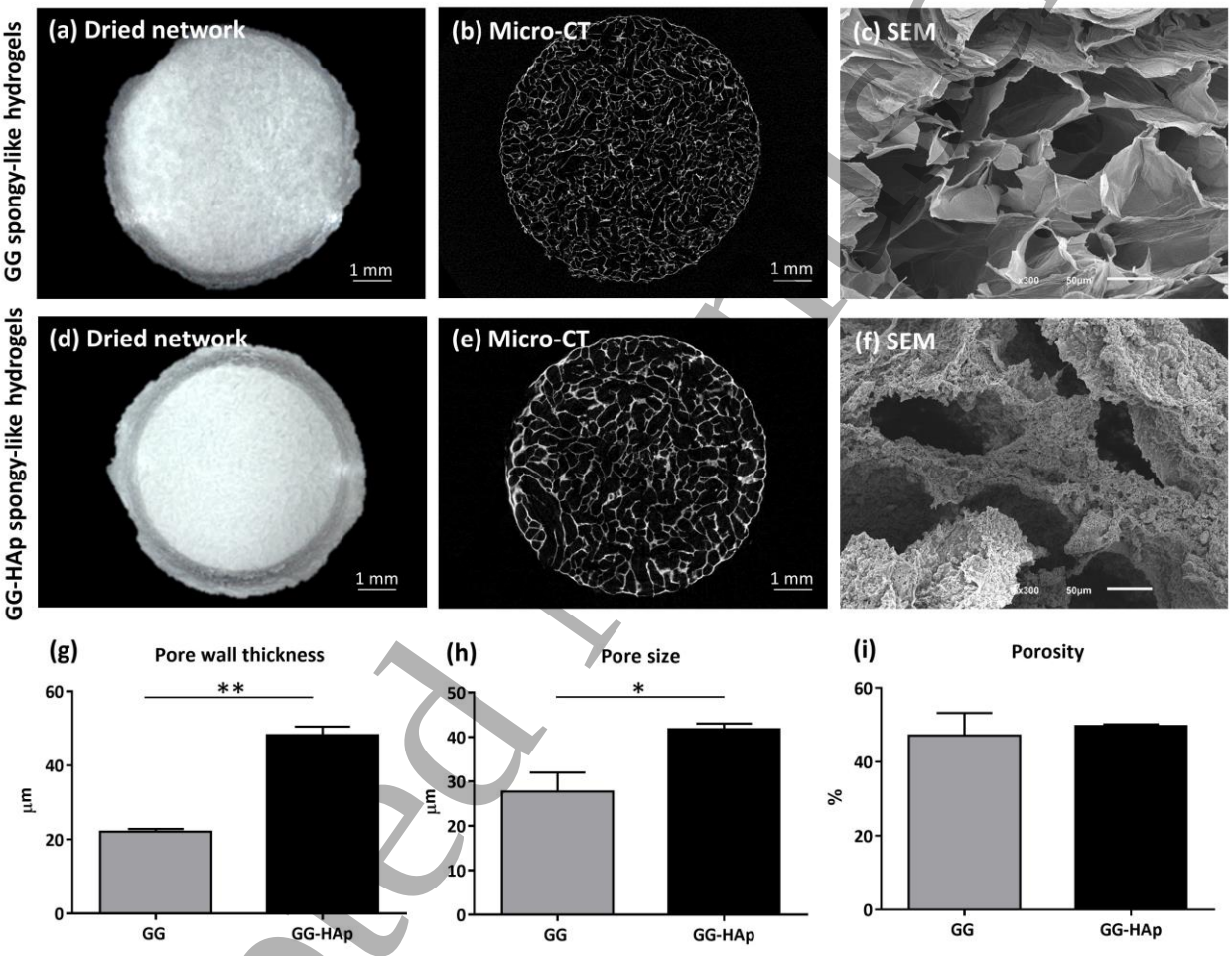

Figure 1. Microstructure of GG and GG-HAp dried polymeric networks analyzed by micro-computed tomography (Micro-CT) and scanning electron microscopy (SEM). (a) GG dried polymeric networks; (b) representative picture of GG dried polymer network obtained by Micro-CT; (c) representative images of topography of GG dried polymer network obtained by SEM; (d) GG-HAp dried polymeric networks; (e) representative picture of GG-HAp dried polymer network

obtained by Micro-CT; (f) representative images of topography of GG-HAp dried polymer network obtained by SEM; (g) average pore wall thickness quantification of GG and GG-HAp dried polymeric networks obtained by Micro-CT analysis; (h) average pore size quantification of GG and GG-HAp dried polymeric networks obtained by Micro-CT analysis; and (i) porosity quantification of GG and GG-HAp dried polymeric networks obtained by Micro-CT analysis; Data is presented as mean±stdev (n=3), (*) denotes statistical differences ($p<0.05$).

3.1.2. *GG and GG-HAp dried polymeric networks' water uptake and mechanical properties*

GG and GG-HAp dried polymeric networks were also analyzed in terms of water uptake and mechanical properties (Figure 2). The water uptake profile of dried polymeric networks, immersed for up to 48h in PBS, was analyzed (Figures 2(a), (b)). As depicted in Figure 2(a), GG and GG-HAp dried polymeric networks reached a maximum of rehydration in the first few minutes of immersion (<30 min.). Furthermore, GG-HAp spongy hydrogels showed six times lower water retention capability than GG spongy-like hydrogels (Figures 2(a), (b)).

The influence of HAp on mechanical properties of swollen GG spongy-like hydrogels was analyzed by DMA (Figures 2(c), (d)). As shown in Figure 2(c) the compressive storage modulus (E', elastic component) was affect by the addition of HAp. In fact, GG-HAp spongy-like hydrogels presented a storage modulus that was twice higher than that of GG spongy-like hydrogels. Additionally, tan δ measurements (Figure 2(d)) revealed that the GG-HAp spongy-like hydrogels were

predominantly elastic (tan δ ≈ 1), while the GG spongy-like hydrogels were predominantly viscous (tan δ > 1).

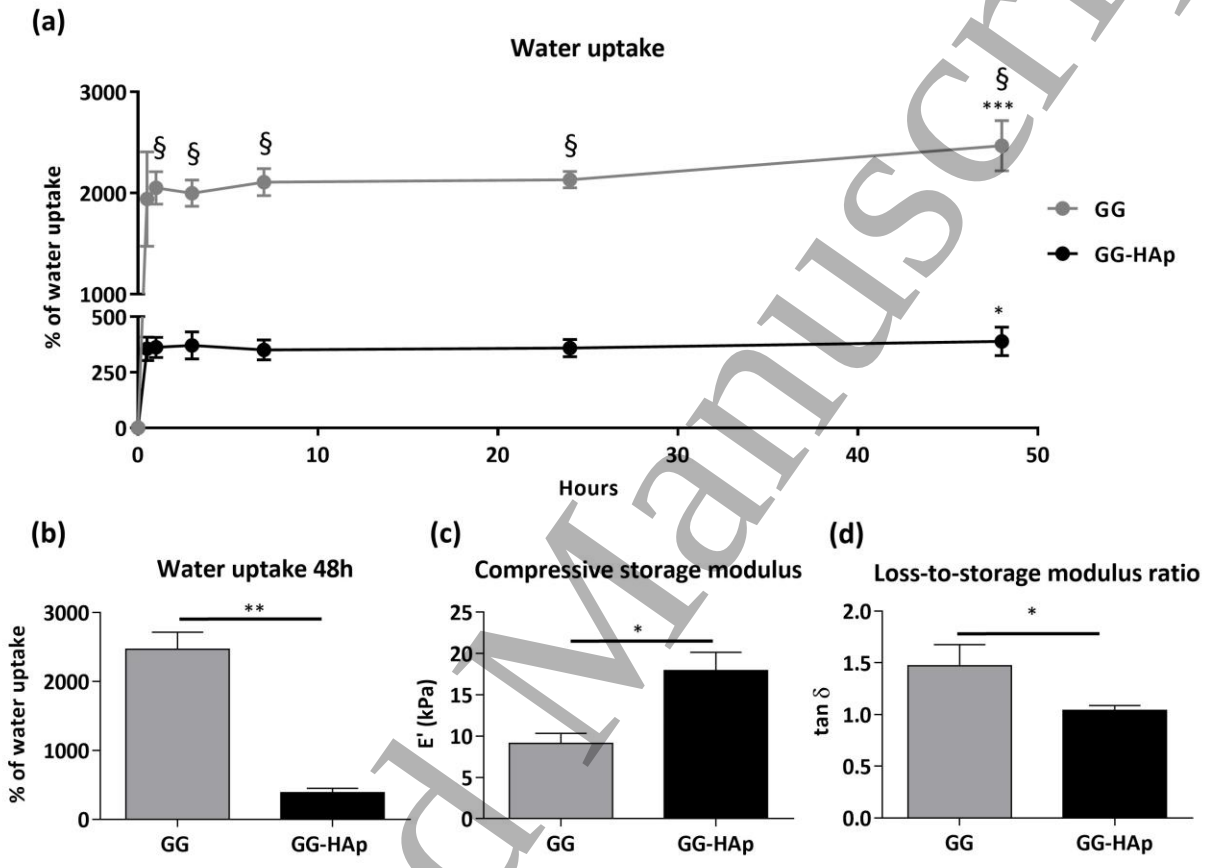

Figure 2. GG and GG-HAp dried polymer networks' water uptake and DMA analyses. (a) GG and GG-HAp dried polymer networks' water uptake along 48 hours of incubation in PBS. Symbols denote statistically significant differences ($p < 0.05$) in comparison to: (§) GG-HAp dried polymer networks, (*) 0 hours; (b) GG and GG-HAp dried polymer networks' water uptake at 48 hours of incubation in PBS. (*) denotes statistical differences ($p<0.05$); (c) average values for the compressive storage modulus (*E'*, elastic component) of swollen GG and GG-HAp spongy-like hydrogels at 1 Hz; and (d) average values for the tan δ (loss-to-storage modulus ratio) of swollen

GG and GG-HAp spongy-like hydrogels at 1Hz. (*) denotes statistical differences ($p<0.05$). Data is presented as mean±stdev (n=3).

3.2. The effects of GG and GG-HAp spongy-like hydrogels on the development of multinucleated TRAP positive (TRAP+) cells

BM cell differentiation into osteoclasts was initially assessed by TRAP staining (Figure 3). The osteoclastogenic potential of isolated BM cells was initially confirmed in 2D standard conditions. After 7 days of culture without and with Vitamin D3 supplementation (Figures 3(a) and 3(b), respectively), TRAP staining was used to visualize the cells and verify the presence of multinucleated cells (more than 3 nuclei). Multinucleated TRAP positive ($TRAP^+$) cells were formed only in the presence of Vitamin D3 (Figure 3(b), inset). In order to investigate the development of osteoclast-like cells in GG and GG-HAp spongy-like hydrogels, BM cells were cultured in the spongy-like hydrogels with and without Vitamin D3 supplementation and stained for TRAP. A number of $TRAP^+$ cells were present in the spongy-like hydrogels, however, the cells were not multinucleated and did not appear to be dependent on Vitamin D3 supplementation (Figures 3(c), 3(d), 3(e) and 3(d)). Interestingly, cell agglomerates composed of $TRAP^+$ cells (Figure 3(e), inset) were only present in GG-HAp spongy-like hydrogels cultured with Vitamin D3.

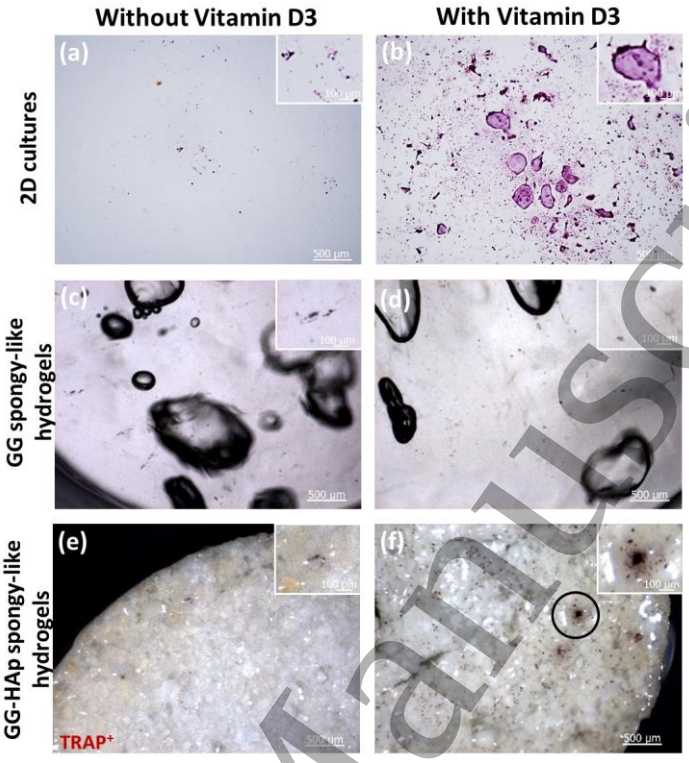

Figure 3. TRAP staining of BM cells cultured for 7 days without and with Vitamin D3. (a) TRAP$^+$ cells in 2D cultures in absence of Vitamin D3 (the inset shows cells at higher magnification); (b) TRAP$^+$ cells in 2D cultures in presence of Vitamin D3 (the inset shows TRAP$^+$ multinucleated osteoclasts); (c) TRAP$^+$ cells cultured in GG spongy-like hydrogels in absence of Vitamin D3; (d) TRAP$^+$ cells cultured in GG spongy-like hydrogels in presence of Vitamin D3; (e) TRAP$^+$ cells cultured in GG-HAp spongy-like hydrogels in absence of Vitamin D3; and (f) Cellular agglomerate of TRAP$^+$ cells (indicated by dark circle) cultured in GG-HAp spongy-like hydrogels in presence of Vitamin D3 (the inset shows a cellular agglomerate at higher magnification).

3.3. The effect of GG-HAp spongy-like hydrogels on BM cells metabolic activity and viability

The effect of GG-HAp spongy-like hydrogels on the metabolic activity and viability of BM cells was assessed over 7 days of culture, in the absence and presence of Vitamin D3. Isolated BM cells were cultured in 2D standard cultures as control. AlamarBlue® assay was used to quantify metabolic activity and Live/Dead assay for qualitative evaluation of live (green) and dead (red) cells (Figure 4). As illustrated in Figure 4(a), in 2D cultures, the metabolic activity of BM cells significantly increased along the culture in presence of Vitamin D3. Whereas, cells in 2D cultures without Vitamin D3 had similar metabolic activity on day 4 and 7 (Figure 4(a)). Additionally, at day 7, in 2D cultures with Vitamin D3 supplementation, higher values were observed as compared with 2D cultures without Vitamin D3. In GG-HAp 3D cultures, Vitamin D3 supplementation had no effect on the level of metabolic activity (Figure 4(d)). The higher fluorescent signal measured on day 4 in 3D cultures in comparison to 2D cultures reflects the higher seeding density in 3D. Cell viability was also investigated using Live/Dead stain. No dead (red) cells were visible in either 2D or 3D cultures (Figures 4(b), (c), (e), (f)). Additionally, cells were viable throughout the spongy-like hydrogels as depicted in the cross-section present in Figure 4 (g). Calcein-stained multinucleated cells were present in the 2D cultures treated with Vitamin D3 (Figure 4(c), arrows).

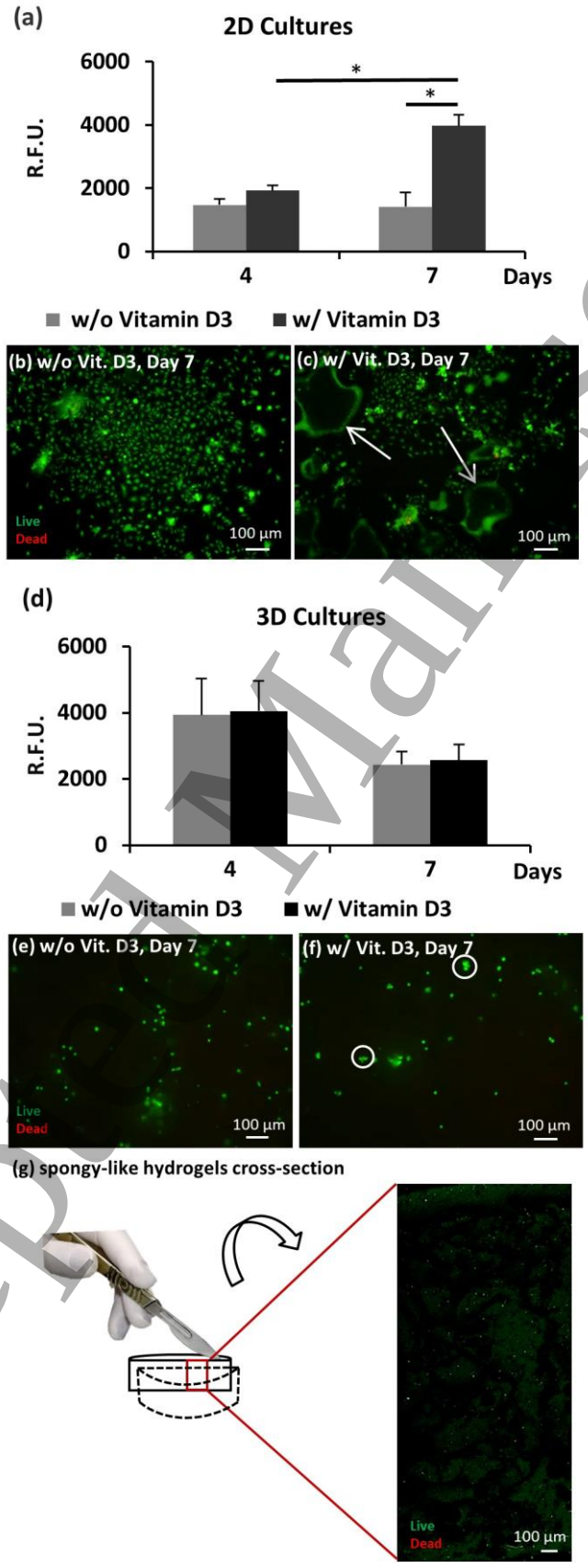

Figure 4. BM cells' metabolic activity and viability during 7 days of culture in presence and absence of Vitamin D3. (a) metabolic activity in 2D cultures in absence and presence of Vitamin D3, as determined by Alamar blue; (b) cell viability of 2D cultures in absence of Vitamin D3; (c) cell viability of 2D cultures in presence of Vitamin D3 (arrows indicate osteoclasts); (d) metabolic activity of 3D cultures (GG-HAp spongy-like hydrogels) in absence and presence of Vitamin D3; (e) cell viability of 3D cultures (GG-HAp spongy-like hydrogels) in absence of Vitamin D3; and (f) cell viability of 3D cultures (GG-HAp spongy-like hydrogels) in presence of Vitamin D3 (white circles indicate cellular agglomerates); (g) representative image of cell viability of spongy-like hydrogel's cross-section. (*) denotes statistical significant differences ($p<0.05$). Data is presented as mean±stdev (n=3).

3.4. The effect of GG-HAp spongy-like hydrogels *on gene expression*

3.4.1. *Osteoclast differentiation*

Gene expression analysis was used to investigate the differentiation of BM cells in GG-HAp spongy-like hydrogels (Figure 5). The markers selected were receptor activator of nuclear factor kappa B ligand (RANKL), osteoprotegerin (OPG), Cathepsin K and dendritic cell-specific transmembrane protein (DC-Stamp). In 2D standard conditions (Figure 5(a) and 5(b)), although not statistically significant it was observed increased RANKL expression and decreased the expression of OPG under Vitamin D3 treatment. In 3D cultures on GG-HAp hydrogels, a similar expression was observed.

The expression levels of Cathepsin K and DC-Stamp were determined due to the fundamental roles of these proteins in osteoclastogenesis and bone resorption. As depicted in Figures 5(c) and 5(d), it was observed that expression levels of Cathepsin K and DC-Stamp were significantly upregulated in 2D cultures with Vitamin D3 supplementation compared with no Vitamin D3 supplementation. Which, additionally, were also higher than 3D cultures within the same conditions. However, in 3D cultures, Cathepsin K and DC-Stamp were expressed at lower levels, which were similar in presence and absence of Vitamin D3.

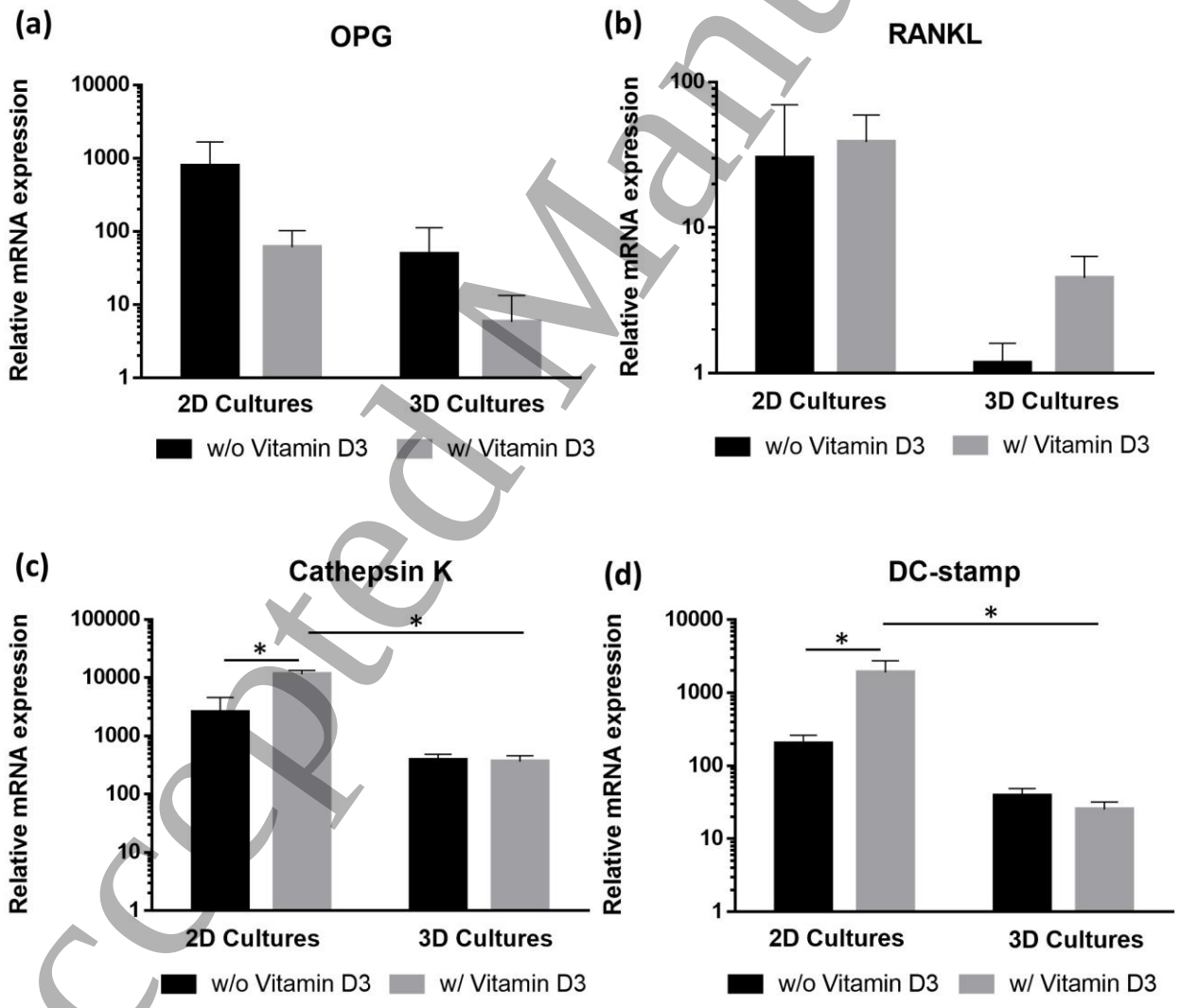

Figure 5. Relative mRNA expression by BM cells cultured during 7 days without and with Vitamin D3 in 2D and 3D (GG-HAp spongy-like hydrogels) cultures. (a) Relative mRNA expression of OPG; (b) Relative mRNA expression of RANKL; (c) Relative mRNA expression of Cathepsin K; and (d) Relative mRNA expression of DC-Stamp. Measures were normalized to 18S expression and are presented in relation to day 0. (*) denotes statistical significant differences ($p<0.05$). Data is presented as mean±stdev (n=3).

3.2.2. Cell cycle

Progenitor cells stop proliferating and go into a quiescence state prior to differentiation. During cell cycle, one of the checkpoints before S-phase is controlled by activation or inhibition of cyclin-dependent kinases (CDK) complexes. Thus, mRNA expression of Cyclin-dependent kinase inhibitors 1a and 1b (Cdkn1a and Cdkn1b) were measured in BM cells in 3D cultures on GG-HAp hydrogels and in 2D control cultures (Figure 6).

As depicted, Cdkn1a and Cdkn1b (Figure 6 (a), (b), respectively) were expressed at similar levels in 2D and 3D cultures. Nevertheless, although, no significant differences were observed in the expression of both inhibitors by cells cultured in the presence and absence of Vitamin D3, it was possible to observe a slight decrease in 2D and 3D cultures with Vitamin D3.

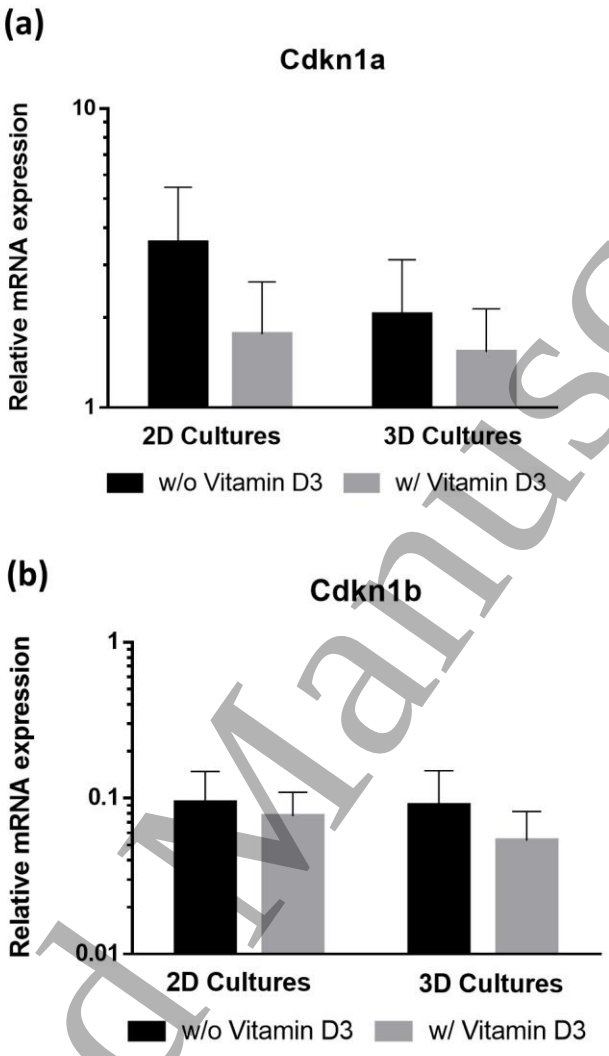

Figure 6. Relative mRNA expression by BM cells cultured during 7 days without and with Vitamin D3 in 2D and 3D cultures (GG-HAp spongy-like hydrogels). (a) Relative mRNA expression of Cdkn1a; (b) Relative mRNA expression of Cdkn1b. Measures were normalized to 18S expression and are presented in relation to day 0. Data is presented as mean±stdev (n=3).

4. Discussion

We have evaluated two biomaterials, GG and GG-HAp spongy-like hydrogels, to be used in bone tissue engineering strategies, but in opposite to the majority of works found in the literature we focus in the support of osteoclasts development from isolated BM cells. In fact, considering a successful biomaterial for bone replacement, it should provide not only support to osteoblasts but also osteoclasts to enable the interactive process of bone remodeling. The results suggests that the reinforcement of GG spongy-like hydrogels with HAp, improved matrices characteristics, which shows to allow the differentiation of BM cells into pre-osteoclasts, in opposite to GG spongy-like hydrogels.

It is known that matrices characteristics influences drastically cells fate. In fact, the microstructure, namely pore size, affects cell migration, nutrient and waste exchange, neovascularization/angiogenesis and bone ingrowth, while water uptake influences biomaterials' ability to absorb body fluids and to transfer nutrients and metabolites. Additionally, it has been shown that the topography of matrices can regulate osteoblasts responses and osteoclastic activity [1]. HAp was chosen to modulate cell's behavior, not only due to their similarity to the mineral found in bone, but also because it has been shown great promises for tissue applications [34]. As expected, the addition of HAp into the GG spongy-like hydrogels resulted into rugged surfaces, higher pore sizes, thicker pore walls, and controlled water uptake, as compared to GG spongy-like hydrogels [23, 35]. In a previous work da Silva L.P. and colleagues have shown that by varying the composition of spongy-like hydrogels precursor solutions, different pore sizes may be obtained [23]. The reason for the change in pore size relates to the freezing point of the solutions, with larger ice crystals, resulting in larger pores formation. This allowed to fine tune the scaffolds accordingly with the final approach. In the case of bone tissue regeneration, it was

shown that pores with a range from ≈ 100 to 300 µm resulted in higher osteoinduction [36]. Whereas, pores with less than 100 µm resulted in hypoxic conditions, which favored osteochondral regeneration. Although, the addition of HAp endorsed the increase of pore size, from ≈ 27 µm in GG spongy-like hydrogels to ≈ 42 µm in GG-HAp spongy-like hydrogels, it was still smaller than 100 µm. Nevertheless, these main observations were achieved with GG and GG-HAp dried polymeric networks, which do not corresponds to the real microstructure of swollen spongy-like hydrogels. Once the spongy-like hydrogels reached their maximum capacity of water uptake, the pore size would increase, reaching the values necessary for osteoinduction.

Concerning, the influence of HAp addition in the water uptake, it might hinder the water uptake due to a decrease of chain flexibility promoted by the electrostatic interactions between the polymer chains and the HAp, as observed for other polymers [37]. Noteworthy, the rapid water uptake observed for both matrices indicates a rapid exchange of nutrients and metabolites. Other important characteristic is the mechanical properties presented by developed scaffolds. Upon dynamic mechanical analysis, it was observed that the addition of HAp resulted in predominantly elastic matrices, which ultimately, would show improved capacity to withstand applied loads and resist fracture.

To evaluate the influence of these characteristics in the support of osteoclast development, matrices were laden with isolated BM cells.

As osteoclast develop, they secret enzymes that digest the extracellular matrix. TRAP is one of the digestive enzymes secreted and is commonly used as an indicator of osteoclast development [38]. TRAP expression can be demonstrated at early stages of osteoclast development in mononuclear cells and at later stages of osteoclastogenesis when cells fuse to form TRAP positive

multinucleated cells, as observed in 2D cultures [39]. Worth mentioning, multinucleated TRAP positive ($TRAP^+$) cells were formed only in the presence of Vitamin D3 [33]. Nevertheless, in 3D culture, no multinucleated $TRAP^+$ cells were observed. In this condition, only aggregates of $TRAP^+$ mononuclear cells were observed. As cell-cell contact is the first step in the process of cell fusion in the formation of multinucleated osteoclasts, it is possible that the cell aggregates visible in GG-HAp spongy-like hydrogels were in very early stages of osteoclastogenesis. The absence of cell aggregates in the GG spongy-like hydrogels suggested that due to its physicochemical characteristics, these matrices were less suitable than GG-HAp spongy-like hydrogels to support osteoclastogenesis, and therefore only GG-HAp spongy-like hydrogels were used for subsequent investigations. Additionally, the global physicochemical characteristics of GG-HAp spongy-like hydrogels, as the higher pore size, lower water uptake and improved mechanical properties, supported this decision.

At this point, metabolic activity and viability of BM cells were evaluated. The higher metabolic activity was detected in the presence of Vitamin D3. This may be related to cell differentiation along the osteoclastogenesis pathway, as shown in a recent work of Lemma S and colleagues, who found an increase of mitochondrial metabolism along with osteoclast differentiation [40]. However, as the bone marrow cultures contain a heterogeneous cell population, the possibility that other cell types contribute to the increased metabolic activity cannot be ruled out. Cell viability was investigated using Live/Dead stain in order to determine whether the lack of effect of Vitamin D3 on the metabolic activity in 3D cultures was due to cell death in the GG-HAp spongy-like hydrogels and no dead cells were visible in either 2D or 3D cultures as observed previously in the literature [41]. Noteworthy, despite the similar values of R.F.Us presented by

2D cultures under Vitamin D3 after 7 days and 3D cultures after 4 days, a great difference was observed in Live/Dead stain images concerning relative cells' confluence. This can be justified by cell migration along the 3D matrices resulting in a higher distribution (less agglomeration) when compared with 2D culture (further details are provided in the Supplementary Information, Figure S1).

Additionally, to confirm cell differentiation, gene expression was analyzed. The markers selected were receptor activator of nuclear factor kappa B ligand (RANKL), osteoprotegerin (OPG), Cathepsin K and dendritic cell-specific transmembrane protein (DC-Stamp). RANKL and OPG are key regulators of osteoclastogenesis produced by osteoblasts/stromal stem cells [42]. The binding of RANKL to its receptor, RANK, which is expressed on osteoclast membranes, is necessary for osteoclast differentiation and survival [43], while OPG is a secreted decoy receptor that binds RANKL and inhibits the RANKL-RANK interaction [44]. In fact, in 3D cultures on GG-HAp hydrogels, although not statistically significant, it was observed that the mean values of RANKL expression were slightly higher and that the mean values of OPG expression were slightly lower, in cultures under Vitamin D3 treatment.

Moreover, although not directly comparable, due to the inherent differences between 2D and 3D culture environments, it is important to notice that the relative expression levels of RANKL and OPG were lower in 3D cultures, than in 2D cultures. This difference could indicate that the proportion of cells of mesenchymal origin is lower in 3D cultures, or that they are in different stages of differentiation in comparison to cell in 2D cultures, and express lower levels of OPG and RANKL. Further studies would be required to explore these possibilities. Additionally, the expression levels of Cathepsin K and DC-Stamp were determined due to the fundamental roles

of these proteins in osteoclastogenesis and bone resorption. Cathepsin K is secreted by osteoclasts during the resorption process [45], while DC-Stamp is essential for cell-cell fusion and multinucleated cells development [39]. Once more, lower levels of these genes expression was observed in 3D cultures, as compared to 2D cultures. The lower expression levels are consistent with the appearance of aggregates of $TRAP^+$ cells in these cultures (Figure 3(f)), in contrast to the fused, multinucleated cells that can be seen in 2D cultures (Figure 3(b)). The lower levels of expression of Cathepsin K in 3D cultures is also indicative of the absence of late-stage osteoclasts. Finally, the cell cycle was analyzed to detect when progenitor cells stop proliferating and go into a quiescence state to undergo into a differentiation pathway. During cell cycle, one of the checkpoints before S-phase is controlled by activation or inhibition of cyclin-dependent kinases (CDK) complexes. Cyclin-dependent kinase inhibitors (Cdkn) can control CDK and are associated with cell cycle arrest and differentiation induction in many different tissue and cell systems. In fact, previous studies demonstrated that a temporal cell cycle arrest is important for osteoclastogenesis progression. For example, it was shown that Cdkn1a and Cdkn1b were expressed in osteoclasts progenitor cells under RANKL presence, while in its absence osteoclasts development was blocked [46]. *In vivo* studies showed that the double knockdown of Cdkn1a and Cdkn1b in mice resulted in less osteoclasts and lower levels of TRAP activity. Additionally, bone marrow derived cells isolated from double knockdown mice showed low TRAP and Cathepsin K expression [47].

Interestingly, Cdkn1a and Cdkn1b were expressed by cells in both culture conditions, indicating that the low levels of Cathepsin K in 3D cultures were not due to the lack of Cdkn1a and Cdkn1b expression. Additionally, it might indicate that cells were in a quiescent state in both cultures and

were differentiating. Nevertheless, since bone marrow contains a mixed cell population, the levels of Cdkn1a and Cdkn1b are not necessarily indicative of osteoclast differentiation. It is important to mention that in previous studies, osteoclasts showed a higher development when cultured in HAp surfaces as they better mimic the mineralized matrix of bone [15]. However, these results were seen in cells cultured for 21 days, as opposed to the 7 days used during the present study.

Our study was limited by the fact that we only found Vitamin D3-dependent aggregates of $TRAP^+$ cells but were not able to demonstrate the formation of multinucleated cells in the spongy-like hydrogels. We followed a protocol of 7 day culture, which had been developed previously using 2D plastic surfaces. It is possible that the differentiation of osteoclasts in 3D is slower than in 2D and therefore a longer incubation period is required for the formation of multinucleated cells. Incubation of up to 21-days of bone marrow cells on the spongy-like hydrogels will be examined in future studies.

5. Conclusions

In the present study, it was shown GG-HAp spongy-like hydrogels present some improved features comparing with GG spongy-like hydrogels: larger pore size, lower water uptake and improved mechanical properties with improved capacity to withstand the applied loads and resist fracture. These features contributed to the successful culture of BM isolated cells on the 3D environment provided by GG-HAp spongy-like hydrogels. Cells growing in the hydrogels were viable, formed aggregates of TRAP-positive cells and expressed the osteoclasts gene markers

Cathepsin K and DC-Stamp. Altogether, results present herein confirm the suitability of GG-HAp spongy-like hydrogels as a new biomaterial for bone tissue regeneration applications.

Acknowledgements

This work was developed under the scope of the European Project skelGEN (Project No: 318553). F.R. Maia acknowledges ERC-2012-ADG 20120216-321266 (ComplexiTE) for her Postdoc scholarship and Boehringer Ingelheim Fonds for her travel grant. L. P. da Silva acknowledges Portuguese Foundation for Science and Technology (FCT) for her grant (SFRH/BD/78025/2011), J. M. Oliveira thanks FCT for his distinction attributed under the FCT Investigator program (IF/00423/2012 and IF/01285/2015). VM Correlo acknowledges Investigator FCT program (IF/01214/2014).

Conflict of interest

The authors declare no conflict of interest.

References

[1] Costa D O, Prowse P D, Chrones T, Sims S M, Hamilton D W, Rizkalla A S and Dixon S J 2013 The differential regulation of osteoblast and osteoclast activity by surface topography of hydroxyapatite coatings *Biomaterials* **34** 7215-26

[2] Douglas T E, Wlodarczyk M, Pamula E, Declercq H A, de Mulder E L, Bucko M M, Balcaen L, Vanhaecke F, Cornelissen R, Dubruel P, Jansen J A and Leeuwenburgh S C 2014 Enzymatic mineralization of gellan gum hydrogel for bone tissue-engineering applications and its enhancement by polydopamine *Journal of tissue engineering and regenerative medicine* **8** 906-18

[3] Jeon O H, Panicker L M, Lu Q, Chae J J, Feldman R A and Elisseeff J H 2016 Human iPSC-derived osteoblasts and osteoclasts together promote bone regeneration in 3D biomaterials *Scientific reports* **6** 26761
[4] Yu X, Tang X, Gohil S V and Laurencin C T 2015 Biomaterials for Bone Regenerative Engineering *Advanced healthcare materials* **4** 1268-85
[5] Yuan X, Wei Y, Villasante A, Ng J J D, Arkonac D E, Chao P-h G and Vunjak-Novakovic G 2017 Stem cell delivery in tissue-specific hydrogel enabled meniscal repair in an orthotopic rat model *Biomaterials* **132** 59-71
[6] Maia F R, Barbosa M, Gomes D B, Vale N, Gomes P, Granja P L and Barrias C C 2014 Hydrogel depots for local co-delivery of osteoinductive peptides and mesenchymal stem cells *Journal of Controlled Release* **189** 158-68
[7] Ribeiro V P, Silva-Correia J, Nascimento A I, da Silva Morais A, Marques A P, Ribeiro A S, Silva C J, Bonifácio G, Sousa R A, Oliveira J M, Oliveira A L and Reis R L 2017 Silk-based anisotropical 3D biotextiles for bone regeneration *Biomaterials* **123** 92-106
[8] Vo T N, Shah S R, Lu S, Tatara A M, Lee E J, Roh T T, Tabata Y and Mikos A G 2016 Injectable dual-gelling cell-laden composite hydrogels for bone tissue engineering *Biomaterials* **83** 1-11
[9] Bar-Shavit Z 2007 The osteoclast: a multinucleated, hematopoietic-origin, bone-resorbing osteoimmune cell *Journal of cellular biochemistry* **102** 1130-9
[10] Detsch R and Boccaccini A R 2015 The role of osteoclasts in bone tissue engineering *Journal of tissue engineering and regenerative medicine* **9** 1133-49
[11] Costa-Rodrigues J, Fernandes A, Lopes M A and Fernandes M H 2012 Hydroxyapatite surface roughness: complex modulation of the osteoclastogenesis of human precursor cells *Acta biomaterialia* **8** 1137-45
[12] Taylor J C, Cuff S E, Leger J P, Morra A and Anderson G I 2002 In vitro osteoclast resorption of bone substitute biomaterials used for implant site augmentation: a pilot study *The International journal of oral & maxillofacial implants* **17** 321-30
[13] Pioletti D P and Kottelat A 2004 The influence of wear particles in the expression of osteoclastogenesis factors by osteoblasts *Biomaterials* **25** 5803-8
[14] Miyatake N, Kishimoto K N, Anada T, Imaizumi H, Itoi E and Suzuki O 2009 Effect of partial hydrolysis of octacalcium phosphate on its osteoconductive characteristics *Biomaterials* **30** 1005-14
[15] Detsch R, Mayr H and Ziegler G 2008 Formation of osteoclast-like cells on HA and TCP ceramics *Acta biomaterialia* **4** 139-48
[16] Jiao K, Niu L N, Li Q H, Chen F M, Zhao W, Li J J, Chen J H, Cutler C W, Pashley D H and Tay F R 2015 Biphasic silica/apatite co-mineralized collagen scaffolds stimulate osteogenesis and inhibit RANKL-mediated osteoclastogenesis *Acta biomaterialia* **19** 23-32
[17] Jones G L, Motta A, Marshall M J, El Haj A J and Cartmell S H 2009 Osteoblast: osteoclast co-cultures on silk fibroin, chitosan and PLLA films *Biomaterials* **30** 5376-84
[18] Naskar D, Ghosh A K, Mandal M, Das P, Nandi S K and Kundu S C 2017 Dual growth factor loaded nonmulberry silk fibroin/carbon nanofiber composite 3D scaffolds for in vitro and in vivo bone regeneration *Biomaterials* **136** 67-85

[19] Jansson P-E, Lindberg B and Sandford P A 1983 Structural studies of gellan gum, an extracellular polysaccharide elaborated by Pseudomonas elodea *Carbohydrate Research* **124** 135-9
[20] Funami T, Noda S, Nakauma M, Ishihara S, Takahashi R, Al-Assaf S, Ikeda S, Nishinari K and Phillips G O 2008 Molecular structures of gellan gum imaged with atomic force microscopy in relation to the rheological behavior in aqueous systems in the presence or absence of various cations *Journal of agricultural and food chemistry* **56** 8609-18
[21] Miyoshi E, Takaya T and Nishinari K 1995 Effects of salts on the gel-sol transition of gellan gum by differential scanning calorimetry and thermal scanning rheology *Thermochimica Acta* **267** 269-87
[22] Stevens L R, Gilmore K J, Wallace G G and in het Panhuis M 2016 Tissue engineering with gellan gum *Biomaterials Science* **4** 1276-90
[23] da Silva L P, Cerqueira M T, Sousa R A, Reis R L, Correlo V M and Marques A P 2014 Engineering cell-adhesive gellan gum spongy-like hydrogels for regenerative medicine purposes *Acta biomaterialia* **10** 4787-97
[24] Coutinho D F, Sant S V, Shin H, Oliveira J T, Gomes M E, Neves N M, Khademhosseini A and Reis R L 2010 Modified Gellan Gum hydrogels with tunable physical and mechanical properties *Biomaterials* **31** 7494-502
[25] Jahromi S H, Grover L M, Paxton J Z and Smith A M 2011 Degradation of polysaccharide hydrogels seeded with bone marrow stromal cells *Journal of the mechanical behavior of biomedical materials* **4** 1157-66
[26] Lee H, Fisher S, Kallos M S and Hunter C J 2011 Optimizing gelling parameters of gellan gum for fibrocartilage tissue engineering *Journal of biomedical materials research. Part B, Applied biomaterials* **98** 238-45
[27] Gantar A, da Silva L P, Oliveira J M, Marques A P, Correlo V M, Novak S and Reis R L 2014 Nanoparticulate bioactive-glass-reinforced gellan-gum hydrogels for bone-tissue engineering *Materials science & engineering. C, Materials for biological applications* **43** 27-36
[28] Jamshidi P, Chouhan G, Williams R L, Cox S C and Grover L M 2016 Modification of gellan gum with nanocrystalline hydroxyapatite facilitates cell expansion and spontaneous osteogenesis *Biotechnology and bioengineering* **113** 1568-76
[29] Vieira S, Vial S, Maia F R, Carvalho M, Reis R L, Granja P L and Oliveira J M 2015 Gellan gum-coated gold nanorods: an intracellular nanosystem for bone tissue engineering *RSC Advances* **5** 77996-8005
[30] Oliveira J T, Gardel L S, Rada T, Martins L, Gomes M E and Reis R L 2010 Injectable gellan gum hydrogels with autologous cells for the treatment of rabbit articular cartilage defects *Journal of orthopaedic research : official publication of the Orthopaedic Research Society* **28** 1193-9
[31] Silva-Correia J, Gloria A, Oliveira M B, Mano J F, Oliveira J M, Ambrosio L and Reis R L 2013 Rheological and mechanical properties of acellular and cell-laden methacrylated gellan gum hydrogels *Journal of biomedical materials research. Part A* **101** 3438-46
[32] Cornish J, Callon K E, Bava U, Kamona S A, Cooper G J and Reid I R 2001 Effects of calcitonin, amylin, and calcitonin gene-related peptide on osteoclast development *Bone* **29** 162-8
[33] Bar-Shavit Z, Teitelbaum S L, Reitsma P, Hall A, Pegg L E, Trial J and Kahn A J 1983 Induction of monocytic differentiation and bone resorption by 1,25-

dihydroxyvitamin D3 *Proceedings of the National Academy of Sciences of the United States of America* **80** 5907-11
[34] Yi H, Ur Rehman F, Zhao C, Liu B and He N 2016 Recent advances in nano scaffolds for bone repair **4** 16050
[35] Kaviani Z and Zamanian A 2015 Effect of Nanohydroxyapatite Addition on the Pore Morphology and Mechanical Properties of Freeze Cast Hydroxyapatite Scaffolds *Procedia Materials Science* **11** 190-5
[36] Bružauskaitė I, Bironaitė D, Bagdonas E and Bernotienė E 2016 Scaffolds and cells for tissue regeneration: different scaffold pore sizes—different cell effects *Cytotechnology* **68** 355-69
[37] Sailaja G S, Ramesh P and Varma H K 2006 Swelling behavior of hydroxyapatite-filled chitosan–poly(acrylic acid) polyelectrolyte complexes *Journal of Applied Polymer Science* **100** 4716-22
[38] Kirstein B, Chambers T J and Fuller K 2006 Secretion of tartrate-resistant acid phosphatase by osteoclasts correlates with resorptive behavior *Journal of cellular biochemistry* **98** 1085-94
[39] Yagi M, Miyamoto T, Sawatani Y, Iwamoto K, Hosogane N, Fujita N, Morita K, Ninomiya K, Suzuki T, Miyamoto K, Oike Y, Takeya M, Toyama Y and Suda T 2005 DC-STAMP is essential for cell-cell fusion in osteoclasts and foreign body giant cells *The Journal of experimental medicine* **202** 345-51
[40] Lemma S, Sboarina M, Porporato P E, Zini N, Sonveaux P, Di Pompo G, Baldini N and Avnet S 2016 Energy metabolism in osteoclast formation and activity *The international journal of biochemistry & cell biology* **79** 168-80
[41] Khang G, Lee S K, Kim H N, Silva-Correia J, Gomes M E, Viegas C A, Dias I R, Oliveira J M and Reis R L 2015 Biological evaluation of intervertebral disc cells in different formulations of gellan gum-based hydrogels *Journal of tissue engineering and regenerative medicine* **9** 265-75
[42] Horwood N J, Elliott J, Martin T J and Gillespie M T 1998 Osteotropic agents regulate the expression of osteoclast differentiation factor and osteoprotegerin in osteoblastic stromal cells *Endocrinology* **139** 4743-6
[43] Anderson D M, Maraskovsky E, Billingsley W L, Dougall W C, Tometsko M E, Roux E R, Teepe M C, DuBose R F, Cosman D and Galibert L 1997 A homologue of the TNF receptor and its ligand enhance T-cell growth and dendritic-cell function *Nature* **390** 175-9
[44] Yasuda H, Shima N, Nakagawa N, Mochizuki S I, Yano K, Fujise N, Sato Y, Goto M, Yamaguchi K, Kuriyama M, Kanno T, Murakami A, Tsuda E, Morinaga T and Higashio K 1998 Identity of osteoclastogenesis inhibitory factor (OCIF) and osteoprotegerin (OPG): a mechanism by which OPG/OCIF inhibits osteoclastogenesis in vitro *Endocrinology* **139** 1329-37
[45] Bossard M J, Tomaszek T A, Thompson S K, Amegadzie B Y, Hanning C R, Jones C, Kurdyla J T, McNulty D E, Drake F H, Gowen M and Levy M A 1996 Proteolytic activity of human osteoclast cathepsin K. Expression, purification, activation, and substrate identification *The Journal of biological chemistry* **271** 12517-24
[46] Okahashi N, Murase Y, Koseki T, Sato T, Yamato K and Nishihara T 2001 Osteoclast differentiation is associated with transient upregulation of cyclin-dependent kinase inhibitors p21(WAF1/CIP1) and p27(KIP1) *Journal of cellular biochemistry* **80** 339-45

[47] Sankar U, Patel K, Rosol T J and Ostrowski M C 2004 RANKL coordinates cell cycle withdrawal and differentiation in osteoclasts through the cyclin-dependent kinase inhibitors p27KIP1 and p21CIP1 *Journal of bone and mineral research : the official journal of the American Society for Bone and Mineral Research* **19** 1339-48